Trans Indian Inst Met (2020) 73(3):613–618
https://doi.org/10.1007/s12666-020-01875-2

ORIGINAL ARTICLE

Development of a Multi-phase AlCuTaVW High-Entropy Alloy Using Powder Metallurgy Route and its Mechanical Properties

Ramya Sree Ganji[1] · Koteswararao V. Rajulapati[1] · K. Bhanu Sankara Rao[2]

Received: 15 November 2019 / Accepted: 17 January 2020 / Published online: 4 February 2020

Abstract Equiatomic AlCuTaVW high-entropy alloy (HEA) composition have resulted in a single-phase solid solution with a bcc crystal structure after 25 h of ball milling. Two fcc phases and an ordered B2 phase have evolved during spark plasma sintering at 1523 K. The morphology of sintered disc contains a continuous bright phase and a discontinuous dark phase. The dark phase is detected to be Al-rich. Microhardness of the sintered product is 13 ± 1 GPa, and it is very high compared to other HEAs, conventional ceramics and cermets. A fracture toughness of 8.36 MPa $m^{1/2}$ is measured from the cracks generated along the edges of Vickers indentation.

Keywords High-entropy alloys · Multi-component · Multi-phase · Hardness · Indentation fracture toughness

1 Introduction

For structural engineering applications, not only hardness/strength, adequate fracture toughness is also an important requirement. However, it is well-documented that hardness and fracture toughness are not inclusive properties as one is achieved at expense of the other [1]. With the recent emergence of multi-principal element, high-entropy alloys (HEAs) with all the alloying elements in equal proportions [2–6], there can be possibilities to break this paradox w.r.t hardness and fracture toughness by proper selection of alloying elements. Although several improved mechanical properties have been reported in HEAs [6–8], the studies related to fracture toughness in these novel alloys are scarce despite some efforts [9–12]. Gludovatz et al. [13] studied CoCrFeMnNi in cast form, and its microstructure revealed equiaxed grains after deformation and subsequent annealing treatment. The fracture toughness of 6 μm grain-sized sample using a notch was 200 MPa $m^{1/2}$. Fracture toughness in $Al_{23}Co_{15}Cr_{23}Cu_8Fe_{15}Ni_{15}$ HEA was measured to be about 5.4–5.8 MPa $m^{1/2}$. Seifi et al. [11] studied cast $Al_{0.2}CrFeNiTi_{0.2}$ and $AlCrFeNi_2Cu$ HEAs. The fracture toughness measured using single-edge notch test samples were 33 MPa $m^{1/2}$ and 42 MPa $m^{1/2}$ for respective compositions. Zhang et al. [12] fabricated $FeCoNiCrCuTiMoAlSiB_{0.5}$, a ten-element HEA, using laser solidification process. This alloy displayed a high fracture toughness of 50.9 MPa $m^{1/2}$. Although these HEAs which were prepared by melting and casting route resulted in high fracture toughness, their reported strength values were not that high.

Therefore in an effort to fabricate a new HEA with improved mechanical properties, a combination of refractory elements such as Ta, V and W and low melting elements such as Al and Cu have been chosen. It is expected that in this alloy, refractory elements will contribute to high strength, whereas Al and Cu will impart some toughness into this alloy. With this aim, the present work involves synthesis of the AlCuTaVW HEA in equiatomic ratio by mechanical alloying (MA) process for 25 h, followed by consolidation into bulk components using spark plasma sintering (SPS). Hardness and fracture toughness have been evaluated using Vickers indentation. It is observed that this novel alloy has possessed high hardness and

✉ Koteswararao V. Rajulapati
kvrse@uohyd.ernet.in; kvrse.uoh@gmail.com

[1] School of Engineering Sciences and Technology, University of Hyderabad, Hyderabad 500046, India

[2] Pratt &Whitney Chair, School of Engineering Sciences and Technology, University of Hyderabad, Hyderabad 500046, India

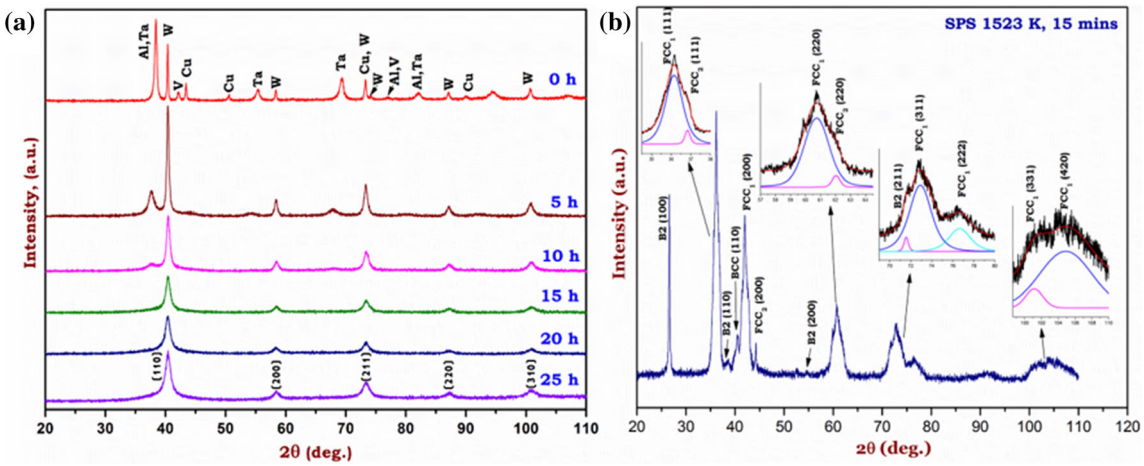

Fig. 1 X-ray diffractograms of AlCuTaVW HEA **a** at different milling times, **b** sintered at 1523 K. The sintering was done using 25-h milled sample. Deconvolution of the peaks is also shown. A single bcc phase obtained after 25 h of ball milling has resulted in the formation of two fcc phases and a B2 phase after SPS

acceptable fracture toughness, thus giving an optimism to develop very strong as well as fracture-resistant engineering alloys using multi-principal element approach.

2 Experimental

Elemental powders of Al, Cu, Ta, V and W (purity > 99%, − 325 mesh) were used as raw materials mixed in equiatomic ratios. High-energy ball milling was done in high-purity argon atmosphere using SPEX 8000D shaker mill. Hardened steel vials and balls were used as the milling media where the ball-to-powder weight ratio was maintained as 5:1. Stearic acid (0.5 wt%) was added as process controlling agent. Milling was carried out for 25 h, and samples were collected at regular intervals of 5 h. The 25-h milled powders were consolidated into bulk material using DR SINTER 1050 apparatus (SPS Syntex Inc., Tokyo, Japan). A preload was applied to make sure that all particles were in contact with each other. Sintering temperature employed was 1523 K under uniaxial load of 80 MPa with a heating rate of 873 K/s. After applying the load and attaining the set temperature, the material was held for 15 min for uniform distribution of the temperature and load. The densities of thus sintered discs were measured using the Archimedes principle method. The MA and SPS processed materials were characterized for phase identification, microstructural evolution and mechanical properties. BRUKER D8 ADVANCE X-ray diffractometer was used; the scan was performed between a 2θ of 20°–110° with a step size of 0.05° and scan rate of 3 s/step. The precise lattice parameter was calculated using the Nelson–Riley extrapolation function. HITACHI S3400N scanning electron microscopy (SEM) coupled with energy dispersive spectroscopy (EDS) was used for microstructural characterization. Walters UHL Vickers microindentation (Model: VMH-I04) was used where a square-based diamond pyramid indenter was employed with an included angle of 136° between opposite faces of pyramid. Hardness was determined at various loads in the range of 100–500 g, at a dwell time of 15 s. Each Vickers hardness value was an average of ten indents taken on a mirror-like surface.

3 Results and Discussion

The X-ray diffractograms obtained from mechanically alloyed powder are shown in Fig. 1a. The XRD pattern of 0-h milling of the alloy blend shows all the elemental peaks. Al and Cu peaks are evident at 0 h but disappears after 5 h of milling indicating the beginning of alloying in this HEA system. This primary dissolution is probably because of the low melting points of Al and Cu and possible interdiffusion of these elements. High intense peak of W element remains stable until 25 h of milling. However, a steep increase in W peak intensity at 40.4° is observed at 5 h of milling, and there is a steady decrease in its intensity thereafter. Twenty-five hour of milling results in a single bcc phase with a lattice parameter of 3.17 Å. The lattice parameter of this newly formed complex, solid solution phase is close to that of W (3.16 Å).

The X-ray diffractogram of the sample sintered at 1523 K is given in Fig. 1b. Sintering at 1523 K temperature results in evolution of new phases. Two fcc phases and an ordered B2 phase have evolved during sintering out of as-milled single-phase bcc structure. The peak reflections

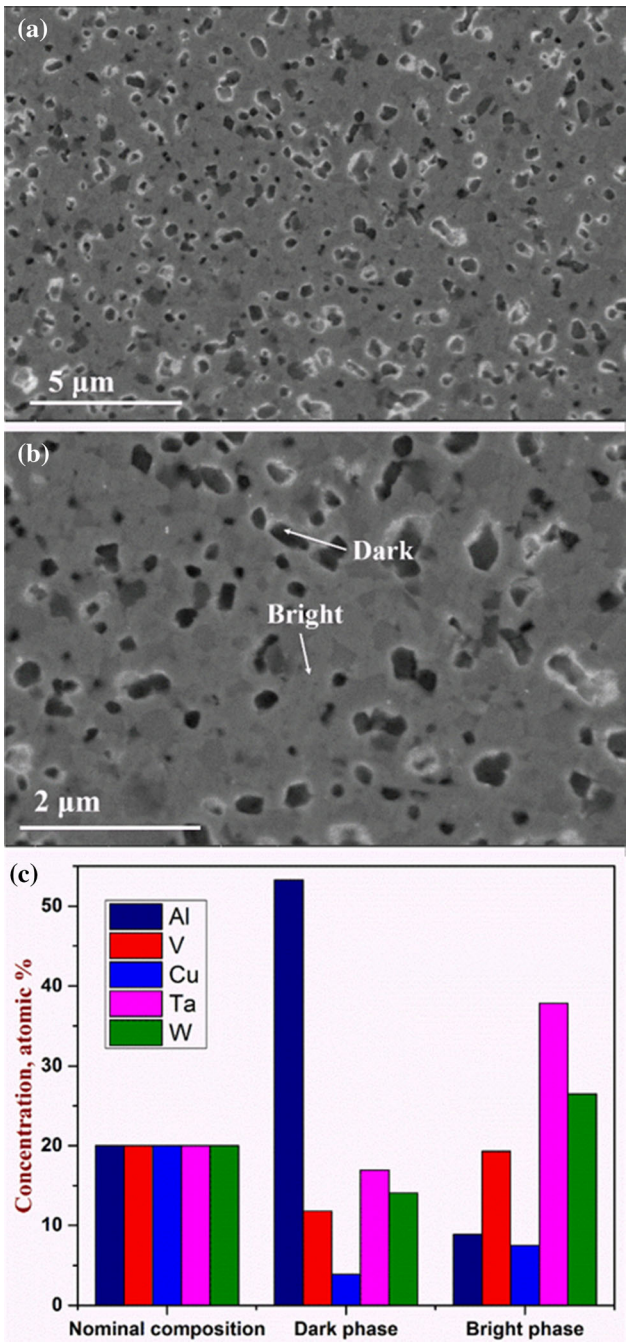

Fig. 2 SEM micrographs of AlCuTaVW HEA sintered **a**, **b** at 1523 K depicting different phases formed during sintering, **c** elemental distribution of dark and bright phases. Bright phase could be a mixture of two fcc phases (fcc1, fcc2) and dark phase could be B2 phase

overlap as the d spacings of different phases are very close to each other. Hence, the peaks are deconvoluted into different phase components. From SEM micrographs, it is observed in Fig. 2a, b that the sample sintered at 1523 K has a continuous bright phase and a discontinuous dark phase homogenously distributed in the bright phase. The EDS analysis shown in Fig. 2c indicates that the dark phase is rich in Al, and the continuous bright phase contains all elements in almost equiatomic ratio with Al deficiency.

Different HEAs developed out of refractory elements have similar microstructural features. Senkov et al. [14] fabricated MoNbTaW and MoNbTaVW using melting and casting process where both the alloys resulted in single bcc phase. Microstructure of the alloys has dendritic and interdendritic regions. The quantitative analysis shows that the W is preferably segregated to dendritic regions, and Mo, V and Nb moved to interdendritic regions in both the alloys. The micro-Vickers hardness values of NbMoTaW and NbMoTaVW HEA are 4.5 GPa and 5.2 GPa, respectively. In another work of Senkov et al. [15] on $CrMo_{0.5}NbTa_{0.5}TiZr$ refractory, HEA produced by melting and casting route, followed by hot isostatic pressing, resulted two bcc phases and one fcc phase. Bcc 1 phase is rich in Nb, Mo and Ta, bcc 2 is rich in Zr and Ti, and fcc is Cr-rich Laves phase because of wide atomic radii difference amongst the participating elements. The Vickers hardness measured is 5.2 GPa, and the compressive yield strength at room temperature is 1.5 GPa. Senkov et al. [16] have fabricated $AlMo_{0.5}NbTa_{0.5}TiZr$ HEA using casting method which have resulted in a bcc phase. The alloy on hot isostatic pressing and annealing treatments transform into a disordered bcc and an ordered B2 phase. The disordered bcc which has a cuboid structure is rich in Mo, Nb, Ta, and precipitation of the ordered B2 solid solution phase is rich in Al, Ti and Zr. AlMoNbTaTiZr demonstrates a very high Vickers microhardness of 5.8 GPa, compression yield strength of 2 GPa, fracture strength of 2.3 GPa and a compression ductility of 10%. Couzinie et al. [17] have fabricated HfNbTaTiZr HEA which also resulted in a bcc structure. The dendritic regions are rich in Nb, Ta and the interdendritic regions have Ti, Zr and Hf.

Vickers microindentation has been performed to understand the bulk mechanical behaviour of AlCuTaVW HEA. The hardness of the of the sample sintered at 1523 K is 13 ± 1 GPa at 100 g load, which is considerably larger in comparison with other refractory HEAs mentioned above.

Fracture toughness values of various HEAs [11, 18] were measured by various methods namely single-edge notched beam, chevron notch or single-edge pre-cracked beam, single-edge V-notched beam and indentation fracture (IF) method. IF method uses the crack lengths generated at the tips of the indentation made by the Vickers indenter. The crack length is inversely proportional to the fracture toughness [19]. The advantage of IF method over other methods is that, there are no prior procedural preparations for the test sample. In general, there are two types of crack formation in IF method. One is Palmqvist crack and other is median/radial/half penny crack. Palmqvist crack spreads on the surface, whereas half penny crack

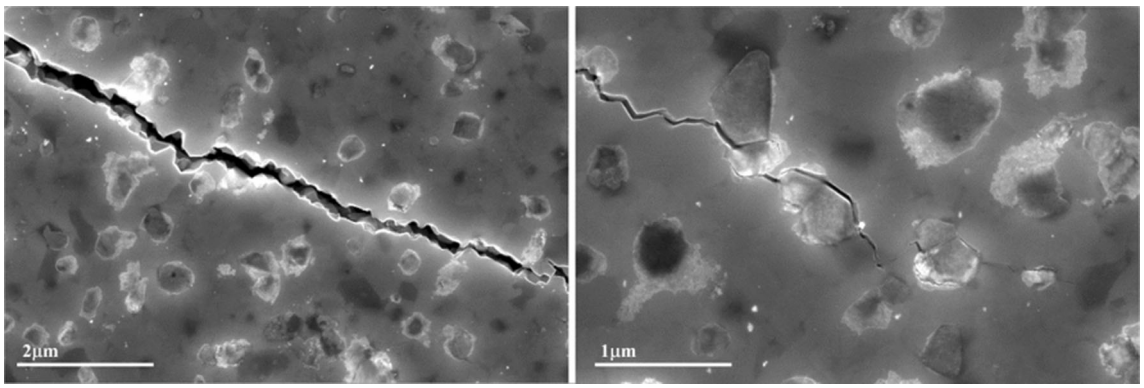

Fig. 3 SEM images of the radial cracks bypassing the dark phase (B2) in specimen (sintered at 1523 K) subjected to Vickers indentation at a load of 3 kg

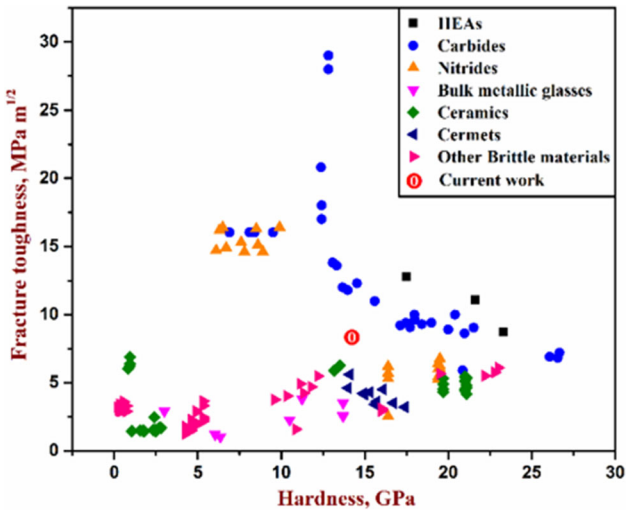

Fig. 4 Indentation fracture toughness values of various structural engineering materials reported in the literature in comparison with present HEA. It is clearly evident that the present HEA possesses both high hardness and high indentation fracture toughness

cuts through the indentation. There are many formulae to estimate the fracture toughness for both the types of cracks [20]. The choice of the formula is based on the type of cracks. Amongst all, the formula proposed in Ref. [21] is widely used to calculate fracture toughness for most of the materials having Palmqvist cracks [20, 22].

In the present study, fracture toughness is measured at 3 kg load using indentation micro-fracture method (IF) on the sintered specimen. Cracks are visible at the indentation tip/edges. All the four crack lengths of the indentation and their diagonal lengths measured from the SEM images have been used to calculate the fracture toughness. In the current investigation, from the micrographs of the indentation, it is identified that the cracks are of Palmqvist type. The indentation fracture toughness, K_{ifr} is calculated using the following formula [21],

$$K_{\mathrm{ifr}} = \frac{1}{3(1-v^2)\left(2^{\frac{1}{2}}\pi\tan\psi\right)^{\frac{1}{3}}}\frac{(HP)^{\frac{1}{2}}}{(4\bar{a})^{\frac{1}{2}}}$$

where H is the hardness of the material in N/m^2, P is the indentation load in N, v is the Poisson's ratio. For bcc materials, Poisson's ratio is 0.33, ψ is the apex or half of face angle of standard Vickers pyramid indenter ($2\psi = 136^\circ$), and $\bar{a}$ is the average radial crack length expressed in m. This formula has been developed to measure the fracture toughness from the Vickers indent crack lengths for brittle materials like WC–Co cermets. Shetty and his co-workers [21] compared different equations using test data of different materials and surprisingly found that Palmqvist cracks model is more suitable than half penny crack model for WC–Co Cermets. However, modelling Palmqvist cracks or radial/median cracks is difficult than the half penny/median/radial cracks. To understand the fracture mechanics, it has been explained by the linear load dependence of crack lengths and the relation of fracture toughness with hardness of the material. It is further assumed that with an increase in load, the Palmqvist cracks prolong on the surface of the material instead of forming a three-dimensional surface crack. The material property ν (Poisson's ratio) and the apex angle $2\psi = 136^\circ$ of Vickers pyramid indenter are also included in the fracture toughness equation. The fracture toughness value of sintered AlCuTaVW HEA containing multi-phase structure has been measured to be 8.36 MPa m$^{1/2}$, and it is relatively high in comparison with majority of hard structural materials. The superior mechanical properties of AlCuTaVW HEA are attributed to the presence of refractory elements in the alloy, solid solution strengthening, interaction between different phases and the ordering of B2 phase in a disordered lattice. The crack propagation in AlCuTaVW alloy is shown in Fig. 3. It is clear from these SEM images that though fracture of the dark phase is observed to a

smaller extent, the crack propagates preferentially bypassing the dark phase.

The fracture toughness of AlCuTaVW HEA is compared with conventional hard materials, and the corresponding compilation is shown in Fig. 4. In this plot, the Vickers hardness is plotted against the fracture toughness measured using the formula given in Ref. [21]. Fracture toughness of various materials plotted are tungsten carbides [23], nitrides [24, 25], bulk metallic glasses [26–28], ceramics [25, 29, 30], cermets and other brittle materials [10, 31–35]. Following the critical evaluation on the indentation fracture toughness data in refs. [36, 37], all the data presented in Fig. 4 have been evaluated using the formula given in Ref. [21]. Figure 4 shows that materials having high fracture toughness are less hard, and the materials with high hardness possess low fracture toughness. It is noteworthy to observe that the hardness of 13 ± 1 GPa and an indentation fracture toughness of 8.36 MPa $m^{1/2}$ are remarkable for the multi-phase HEA developed in the present study. This very high hardness is expected due to the presence of refractory elements in the alloy, ordered as well as multi-phase structure. The high indentation fracture toughness is probably because of the obstruction of crack propagation in the soft fcc matrix by harder B2 particles (Fig. 3).

4 Conclusions

A novel equiatomic AlCuTaVW HEA has been successfully fabricated using the mechanical alloying followed by spark plasma sintering. Microstructural features and mechanical properties of this alloy have been studied in detail. Twenty-five hours of milling has resulted in a single-phase solid solution comprising of a bcc crystal structure. Two fcc phases and an ordered B2 phase have evolved in the alloy after sintering as evidenced in XRD analysis. The Vickers hardness measured at 100-g load for the specimen sintered at 1523 K is 13 ± 1 GPa. These values are superior when compared to other HEAs, ceramics and cermets. Such a high strength is attributed to the presence of high melting materials, solid solution strengthening effects, interaction between different phases and the ordered B2 phase. Fracture toughness of AlCuTaVW alloy is measured as 8.3 MPa $m^{1/2}$. The uniqueness of this work is possession of both high hardness as well as reasonably good indentation fracture toughness by this new multi-phase HEA system, thus providing an optimism towards development of strong as well as fracture-resistant bulk structural engineering alloys using multi-principal element approach.

Acknowledgements DST-PURSE and DST-FIST programs of School of Engineering Sciences and Technology, University of Hyderabad are gratefully acknowledged for supporting this research work. The authors are thankful to Mr. PVV Srinivas of the International Advanced Research Centre for Powder Metallurgy and New Materials (ARCI), Hyderabad 500005, India, for assisting with spark plasma sintering.

References

1. Jones D R H, and Ashby M F, *Engineering Materials 1: An Introduction to Properties, Applications and Design*. 4th Ed., Butterworth-Heinemann, Amsterdam (2009).
2. Yeh J W, Chen S K, Lin S J, Gan J Y, Chin T S, Shun T T, Tsua C H, and Chang S Y, *Adv Eng Mater* **6** (2004) 299.
3. Murty B S, Yeh J W, and Ranganathan S, *High-Entropy Alloys*, Butterworth-Heinemann, Boston (2014).
4. Miracle D B, and Senkov O N, *Acta Mater* **122** (2017) 488.
5. Gao M C, Yeh J W, Liaw P K, and Zhang Y, *High-Entropy Alloys Fundamentals and Applications*, Springer International, Switzerland (2016).
6. Ganji R S, Sai Karthik P, Bhanu Sankara Rao K, and Rajulapati K V, *Acta Mater* **125** (2017) 58.
7. Li Z, Tasan C C, Springer H, Gault B, and Raabe D, *Sci Rep* **7** (2017) 40704.
8. Hsu W -L, Yang Y -C, Chen C -Y, and Yeh J -W, *Intermetallics* **89** (2017) 105.
9. Gludovatz B, Hohenwarter A, Catoor D, Chang E H, George E P, and Ritchie R O, *Science* **345** (2014) 1153.
10. Mallik M, Pan S, and Roy H, *Int J Curr Eng Tech* **3** (2013) 1647.
11. Seifi M, Li D, Yong Z, Liaw P K, and Lewandowski J J, *Jom* **67** (2015) 2288.
12. Zhang H, He Y, and Pan Y, *Scr Mater* **69** (2013) 342.
13. Gludovatz B, George E P, and Ritchie R O, *Jom* **67** (2015) 2262.
14. Senkov O N, Wilks G B, Miracle D B, Chuang C P, and Liaw P K, *Intermetallics* **18** (2010) 1758.
15. Senkov O N, and Woodward C F, *Mater Sci Eng A* **529** (2011) 311.
16. Senkov O, Isheim D, Seidman D, and Pilchak A, *Entropy* **18** (2016) 102.
17. Couzinié J P, Dirras G, Perrière L, Chauveau T, Leroy E, Champion Y, and Guillot I, *Mater Lett* **126** (2014) 285.
18. Zhang A, Han J, Su B, Li P, and Meng J, *Mater Des* **114** (2017) 253.
19. Strecker K, Ribeiroa S, and Hoffmannb M -J, *Mater Res* **8** (2005) 121.
20. Bouteghmes D, Hamidouche M, and Bouaouadja N, *Int Rev Mech Eng* **6** (2012) 803.
21. Shetty D K, Wright I G, Mincer P N, and Clauer A H, *J Mater Sci* **20** (1985) 1873.
22. Spiegler R, Schmauder S, and Sigl L S, *J Hard Mater* **1** (1990) 147.
23. Medeiros E E, and Dias A M S, *Int J Recent Res Appl Stud* **17** (2013) 9.
24. Lenka K, Duszová A, Kašiarová M, Dorčáková F, Dusza J, and Balázsi C, *Acta Metall Slovaca* **3** (2013) 213.
25. Sedlák R, Kovalčíková A, Tatarková M, Rutkowski P, and Dusza J, *Defect Diffus Forum* **368** (2016) 166.
26. Abbas S Z, Khalid F A, and Zaigham H, *J Non-Cryst Solids* **457** (2017) 86.
27. Gilbert C J, Ritchie R O, and Johnson W L, *Appl Phys Lett* **71** (1997) 476.
28. Madge S V, *Metals* **5** (2015) 1279.
29. Ćorić D, Ćurković L, Renjo M M, and Famena T, *Transactions of Femena XLI-2* (2017) 1.

30. Andrejovská J, Mihalik J, Kovaľ V, Bruncková H, and Dusza J, *Acta Metall Slovaca* **15** (2009) 112.
31. Min K S, Ardell A J, Eck S J, and Chen F C, *J Mater Sci* **30** (1995) 5479.
32. Balog M, Hric L, Křest'an J, Bača L, and Šajgalík P, *Powder Metall Prog* **6** (2006) 137.
33. Pramanick A K, *Int J Res Eng Tech* **4** (2015) 334.
34. Ballóková B, and Besterci M, *Powder Metall Prog* **8** (2008) 270.
35. Rios C T, Contieri R J, Souza S A, Cremasco A, Hayama A O F, and Caram R, *Mater Des* **33** (2012) 563.
36. Anstis G R, Chantikul P, Lawn B R, and Marshall D B, *J Am Ceram Soc* **64** (1981) 533.
37. Quinn G D, and Bradt R C, *J Am Ceram Soc* **90** (2007) 673.